# Properties of the underwater sound fields during some well documented beaked whale mass stranding events

GERALD L. D'SPAIN*, ANGELA D'AMICO+ AND DAVID M. FROMM#

*Contact e-mail: gld@mpl.ucsd.edu*

ABSTRACT

Recent mass strandings of marine mammals, mostly Cuvier's beaked whales (*Ziphius cavirostris*) from the family of ziphiidae, have occurred coincident in space and time with human production of high levels of underwater sound. Three of these events, the May 1996 mass stranding along the Greek coast, the Bahamas mass stranding event in March 2000 and the September 2002 event in the Canary Islands, were selected for consideration here since pertinent information was readily available. The purpose of this paper is to summarise the probable characteristics of the sound fields during these events and to search for common features. The acoustic sources in all three cases moved at speeds of 5 knots or greater and generated periodic sequences of high amplitude, transient pulses 15-60s apart that contained significant energy in the 1-10kHz frequency band. The environmental conditions included water depths exceeding 1km close to land. In addition, the depth dependence of the ocean sound speed created an acoustic waveguide whose lower boundary was formed by refraction within the water column. The anthropogenic sources in all cases were located within such waveguides. Under these conditions, sound levels decrease more slowly with increasing range after a certain transition range than otherwise, due to sound focusing and to decreased attenuation because of isolation over extended ranges from the ocean bottom. In addition, the frequency dispersion is such that pulses tend to remain as pulses during propagation. For those events involving near-surface sources in surface ducts, weather conditions were calm leading to minimal sound attenuation and scattering by near-surface bubbles and ocean surface roughness. Quantitative prediction of the actual sound field properties during these events is limited primarily by the lack of knowledge of prevailing environmental conditions. Results from simple numerical modelling show that received sound level increases of up to 20dB occur after the transition range for sources and receivers within refractive waveguides. Data-based semi-empirical models of surface duct propagation provide simple, realistic, quantitative estimates of the mean acoustic field in the duct and the effects of changes in environmental conditions. Numerical modelling of total sound exposure (pressure squared integrated with respect to time) illustrates the importance of the relative velocity and minimum range between source and receiver, indicating that realistic animal motion models are required to obtain representative results. Although several features of the sound fields during these three mass stranding events are very similar, their actual relationship to the strandings is unknown.

KEYWORDS: NOISE; STRANDINGS; MODELLING; ACOUSTICS; BEAKED WHALES

## INTRODUCTION

Several authors (e.g. Frantzis, 1998; Anon., 2001; Department of the Environment, 2002) have suggested in recent years that high sound level sonars may be responsible for mass strandings of beaked whales (family Ziphiidae), defined as the strandings of two or more whales other than a cow-calf pair (Cox *et al.*, 2006). Other sources of anthropogenic sound also have been implicated (e.g. Gentry, 2002). Although a cause-and-effect relationship has not been firmly established, several of these human activities are temporally and spatially correlated with mass strandings of Cuvier's beaked whales (*Ziphius cavirostris*) alone or with members of the genus Mesoplodon (e.g. *Mesoplodon densirostris, M. europaeus*). Over the past decade, the public and the scientific community have become increasingly aware that some historical mass strandings of beaked whales also may be associated, both spatially and temporally, with military use of sonar (e.g. Frantzis, 1998; Department of the Environment, 2002; Cox *et al.*, 2005).

Three of the best documented stranding events, for which some information is readily available, are the focus of this paper. These events are: (1) the strandings along the west coast of Greece in May 1996 (D'Amico and Verboom, 1998; Frantzis, 1998); (2) the Bahamas stranding event in March 2000 (Anon., 2001; Fromm and McEachern, 2000); and (3) the Canary Islands stranding event in September 2002 (Department of the Environment, 2002). The 1996 Greek strandings occurred during the same time period that the North Atlantic Treaty Organisation (NATO) SACLANTCEN Undersea Research Centre performed an acoustic experiment called Shallow Water Acoustic Classification in Kyparissiakos Gulf, close to the Greek Coast. The majority of the dozen or so animals stranded in a two-day period (12-13 May) over approximately 35km of coastline (D'Amico and Verboom, 1998).

The Bahamas event consisted of a mass stranding of 16 cetaceans, comprised of both beaked and common minke whales (*Balaenoptera acutorostrata*), over a 240km arc of coastline bordering the Northeast and Northwest Providence Channels of the Bahamas Islands. The strandings occurred over a 36-hour period, 15-16 March 2000 and corresponded simultaneously with the transit of five US Navy surface ships through the channels, operating mid-frequency hull-mounted sonar systems as part of a training exercise. Only detailed information on four of the five US ships is provided by Anon. (2001) and Fromm and McEachern (2000). Based on the way in which the strandings coincided with this naval activity, it was concluded that the tactical mid-range sonars were the most plausible cause of the trauma observed in the autopsies of stranded animals (Anon., 2001).

Over 24-27 September 2002, a mass stranding of approximately 14 cetaceans, all beaked whales (for those animals where species identification was made), occurred along the southeast side of the island of Fuerteventura and the northeast side of Lanzarote in the Canary Islands. This stranding was temporally and spatially coincident with an international naval exercise called Neo Tapon. The exercise

* *Marine Physical Laboratory, Scripps Institution of Oceanography, 291 Rosecrans St., San Diego, CA 92106, USA.*
+ *SPAWAR Systems Center – San Diego, Code 2716, 53560 Hull St., San Diego, CA 92152-5001, USA.*
# *Naval Research Laboratory, Code 7142, 4555 Overlook Ave., S.W., Washington DC, 20375-5350, USA.*

involved ships and aircraft from 11 NATO countries (Socolovsky, 2002). Six mass strandings of beaked whales had previously taken place along these same sections of coastline over the six-year period 1985-1991, many of which were coincident in time with naval exercises in the area (Department of the Environment, 2002). The specifics of the naval activities during Neo Tapon are not readily available. However, military hull-mounted sonar systems similar to those used during the Bahamas event were likely in operation given that surface ships and submarines were participating in 'acoustic exercises' at the time (Department of the Environment, 2002; Table 2).

A common aspect of these three stranding events is that they were coincident in time and space with exercises involving the operation of mid-frequency sonar systems (the Greek event was the only one known to have involved a low frequency sonar in addition to a mid-frequency sonar). Some people have also suggested a link between beaked whale strandings and seismic air gun operations (Gentry, 2002; Cox *et al.*, 2006). For completeness, the general properties of the acoustic signals generated by seismic air gun arrays operated by the oil and gas industry are included in this paper, along with those of the mid-frequency sonars and the low frequency sonar used in Greece.

This paper summarises the probable characteristics of the sound fields during these events and searches for common features. In any discussion of underwater sound fields and marine life, distinctions must be made between the properties of the acoustic source, the properties of the environment (the medium through which the sound travels), the received acoustic field properties at a specified location and the characteristics of an animal's perception of the sound. First, the properties of the acoustic sources that were in operation during these stranding events are summarised followed by a discussion of what is known about the characteristics of the environments in which the strandings occurred. The lack of knowledge of the environmental conditions during the events probably is the source of greatest uncertainty in the prediction of the received acoustic field at a given location. Some of the relevant features of sound propagation in these environmental settings are outlined in this paper. Background information on acoustic propagation modelling and some examples of acoustic propagation modelling to illustrate some of the main points in the paper are also presented. The perception of sound fields by marine mammals is beyond the scope of this paper.

## PROPERTIES OF THE ACOUSTIC SOURCES

### Greece, 1996

The Towed Vertically Directive Source (TVDS) used in the 1996 Shallow Water Acoustic Classification experiment was towed by the NATO Research Vessel *Alliance* at various depths from 60 to 93m, but primarily in the 70-85m depth interval. It differs in this regard from the other sources discussed herein in that it operated at depths greater than 10m. The source transmitted for 2.5 to 3.75hrs during each run, with three runs per day over four consecutive days (D'Amico and Verboom, 1998). Acoustic signals were generated simultaneously in two different frequency bands with centre frequencies of 600Hz and 3kHz and at source levels of 228 and 226dB re: 1μPa at 1m, respectively (Table 1). Both continuous wave (CW) signals (i.e. a tone at a constant, single frequency) and hyperbolic frequency-modulated (HFM) waveforms (where the frequency of the tone being transmitted varies continuously over time with a temporal dependence given by a hyperbola) were used in the tests. CW signals are sensitive to the motion of an acoustic reflector, whereas HFM signals are invariant to reflector motion but instead provide information on the distance to the reflector. The TVDS had a vertical beamwidth of 23° at 600Hz and 20° at 3kHz. These two beams were oriented in the horizontal direction to focus the radiated sound along the axis of the sound channel (discussed later).

Given that the pulses in both frequency bands always were transmitted simultaneously (probably in a phase coherent way) and that the main beams of the vertical source array components for the two frequency bands were oriented in the same direction (horizontal) at all times, then the combined pulses can be considered as one pulse. In this case,

$$\text{coherent (amplitude) addition} = 20\log_{10}\left(10^{228/20}+10^{226/20}\right)$$

therefore, the overall source level = 233dB re: 1μPa at 1m.

$$\text{For incoherent (energy) addition} = 10\log_{10}\left(10^{228/10}+10^{226/10}\right)$$

therefore, the overall source level = 230db re: 1μPa at 1m.

### Bahamas, 2000

The sonars used in the Bahamas event were types AN/SQS 53C and AN/SQS 56 hull-mounted systems. The 53C was used on two ships and transmitted at centre frequencies of 2.6kHz and 3.3kHz. They operated for most of the time at a source level of 235dB re: 1μPa at 1m. The 56 sonars transmitted signals with centre frequencies of 6.8kHz, 7.5kHz and 8.2kHz at 223dB re: 1μPa at 1m source level. During the exercise, these sonars each transmitted pulses of 1-2s in duration once every 24s. Pulse transmissions from each ship were staggered in time to prevent overlap. This 24s interpulse interval allowed reflections from surfaces and objects out to distances approaching 20km from the ship (40km round trip) to be received before the next pulse was transmitted. The pulses had rise times of 0.1-0.4s and typically were comprised of three consecutive waveform types (Table 1), with nominal bandwidths up to 100Hz. Both 53C and 56 sonars are vertically directional. The 53C has a nominal 40° vertical beamwidth (depending upon frequency) centred at 8m depth and which was steered 3° down from horizontal direction. The SQS 56 has a somewhat narrower main lobe of 30°, centred at 6m depth and steered horizontally. Both sonars create acoustic fields that are omnidirectional in azimuth, although the 53C also can create beams covering 120° azimuthal sectors that can be swept from side to side during transit.

### Canary Islands, 2002

Information is not readily available on the types of naval sonars employed during the 2002 Neo Tapon exercise. However, given that at least one aircraft carrier, 50 surface vessels, 6 submarines and 30 aircraft were participating in 'acoustic exercises' at the time of the strandings (Department of the Environment, 2002), it can be reasonably assumed that tactical hull-mounted sonar systems similar to those used during the 2000 Bahamas stranding event were in operation. Table 2 lists the types of surface ship sonar systems used by the navies of the 11 NATO countries reported to have participated in the Canary Islands exercise.

Table 1
Summary of acoustic source properties.

| | TVDS low frequency | TVDS mid frequency | AN/SQS 53C | AN/SQS 56 | Air gun array |
|---|---|---|---|---|---|
| Waveform | HFM/CW[1] | HFM/CW | FM/CW[1] | FM/CW | BB pulse[2] |
| Source level[3] | 228dB[4] | 226dB[4] | 235dB | 223dB | 260dB[5] |
| Pulse duration | 4sec | 4sec | 1-2sec | 1-2sec | 0.02sec |
| Inter-pulse time | 1min | 1min | 24sec | 24sec | 10-12sec |
| Centre frequency | 600Hz | 3,000Hz | 2,600Hz 3,300Hz | 6,800Hz 7,500Hz 8,200Hz | Broadband[6] |
| Bandwidth | 250Hz | 500Hz | 100Hz | 100Hz | Wideband[7] |
| Source depth | 70-85m | 70-85m | 8m | 6m | 6-10m |
| Beamwidth | 23° | 20° | 40° | 30° | Function of freq |
| Beam direction | Horizontal | Horizontal | 3° down from horizontal | Horizontal | Vertical |

[1]Hyperbolic frequency modulated (HFM), continuous wave (CW), and frequency modulated (FM).
[2]Broadband (BB).
[3]The source level is the estimated acoustic pressure level of the radiated sound from a source as measured in the far-field and then back-propagated to a reference distance, usually 1m, from the acoustic center of the source. Source levels (rms for sonars and 0-pk for the air gun array are in units of dB re 1 µPa @ 1m).
[4]The simultaneous low frequency and mid frequency transmissions considered as one pulse have a source level of 233dB re: 1 µPa @ 1m (coherent addition) and 230dB re: 1 µPa @ 1m (incoherent addition).
[5]0-pk source level for an equivalent point source along the main beam in the far field.
[6]Peak levels in the 5-300Hz band.
[7]Radiated acoustic energy extending up to several kHz.

**Seismic airgun arrays**

Air gun arrays are used in seismic reflection surveys to search for oil and gas deposits under the ocean floor. These arrays typically are composed of 12 to 48 air guns that are towed by the survey vessel at 5-10m depth in a horizontally oriented and rectangular geometry with dimensions of approximately 20 × 20m (National Research Council, 2003). The air guns release compressed air simultaneously to create a high level, short duration (20-30ms) sound pulse that is focused in the vertical direction. The air guns are 'fired' once every 10-12s during a survey. The pulse rise times are a few ms and the source levels for an equivalent point source measured in the main beam direction in the far field (i.e. at distances significantly greater than the dimensions of the array) approach 260dB re: 1µPa at 1m zero-to-peak. The pulses usually have maximum energy in the 5-300Hz range, with energy decreasing with increasing frequency. However, it appears that they still contain appreciable energy up to several kilohertz (Fontana, 2002; Diebold *et al.*, 2003).

A summary of the salient features of the sonars used during the 1996 Greek event (the TVDS source described in D'Amico and Verboom, 1998) and during 2000 Bahamas event (the AN/SQS 53C and 56 sonars; Anon., 2001), as well as the air gun arrays reported in National Research Council (2003) is given in Table 1. All ships involved in these events travelled at speeds of 5kt (2.6m $s^{-1}$) or greater during operation.

## PROPERTIES OF THE ENVIRONMENT

The first obvious environmental similarity between these stranding events is that the acoustic source(s) was operated in a region inhabited by beaked whales and within tens of kilometres of land. These regions contain areas with complex, steeply-sloping bathymetry and places where water depths of 1km or greater exist. The ocean regions overlying these types of bathymetric features may be desirable habitats for beaked whales. However, the characteristics of the ocean bottom are of secondary importance in determining the properties of the acoustic fields. The interactions of the sound fields with the ocean bottom appear to have been minimal, except possibly at short ranges from the source(s) and very close to land (where the bathymetry begins to shoal), because of the depth dependence of the water column sound speed. For the case of the sonar systems, bottom interaction also was reduced by the source radiation pattern, which focused the sound in the horizontal direction. For each stranding event, the dependence of the speed of sound on depth (Figs 1 and 2; discussed below) appears to have created a waveguide, or acoustic lens, that focused sound from sources within the waveguide to long ranges, i.e. ranges that approach the distance of the sound source(s) from land. As discussed below, one aspect of waveguide focusing is the change in the rate of geometrical spreading of the sound field from spherical to cylindrical spreading after the transition range, $r_t$, resulting in a decrease in transmission loss in decibels equal to $10\log_{10}(r/r_t)$.

During the 1996 Greek stranding event, the acoustic waveguide was centred at a depth of 85m (Fig. 2, right hand panel), corresponding to the depth of the TVDS deployment (D'Amico and Verboom, 1998). The type of acoustic waveguide present in this environment is formed by the same physical processes that form the acoustic waveguide throughout the deep oceans of the world. That is, it is formed by the combined depth dependence of water temperature and ambient pressure. Temperature typically decreases or remains constant with increasing depth (unless the salt content increases to compensate for the effects on density). In contrast, the ambient pressure, caused by the weight of the overlying water column, monotonically increases with depth. The speed of sound in water decreases with decreasing temperature but increases with increasing pressure, so that the interplay of these two factors creates a deep ocean acoustic waveguide. This deep ocean waveguide, or sound channel, is so important to deep water acoustic propagation that it has been assigned two acronyms, the SOFAR (sound fixing and ranging) channel and the DSC (deep sound channel). The depth of the centre of the deep sound channel is a function of latitude, being deepest in equatorial regions where the surface waters are warm, and ascending to the surface at high latitudes (e.g. Medwin and Clay, 1998). The acoustic waveguide at 85m in

Table 2

Surface ship sonar systems of the 11 NATO countries reportedly participating in Neo Tapon 2002 (Jane's Underwater Warfare Systems, 2004; Friedman, 1989).

| Country | System | Frequency (kHz) | Type[1] | Installed on (class) | Number of units[2] |
|---|---|---|---|---|---|
| Belgium | AN/SQS 510 | 4.3-8 | HM | Wielingen | 3 |
| Canada | AN/SQS 510 | 4.3-8 | HM | Halifax | 12 |
| | | | VDS/HM | Iroquois | 4 |
| France | DUBA 25 | 8-10 | HM | Type A69 | 9 |
| | | | | Cassard | 1 |
| | DUBV 23 | 4.9-5.4 | HM | Suffren | 1 |
| | | | | Tourville | 2 |
| | | | | Georges Leygues | 4 |
| | DUBV 24 | 4.9-5.4 | HM | Cassard | 1 |
| | | | | Georges Leygues | 3 |
| | | | | Jeanne d'Arc | 1 |
| | DUBV 25 | 4.9-5.4 | HM | Cassard | 1 |
| | DUBV 43B/C | 5 | VDS | Suffren | 1 |
| | | | | Georges Leygues | 7 |
| Germany | DSQS 21 | In the band 3-14 | HM | Bremen | 8 |
| | | | | Lutjens | 1 |
| Greece | 1 BV | Greater than 14 | HM | Thetis | 5* |
| | AN/SQS 56 (DE 1160[#]) (DE 1164) | 6.7 - 8.4 | HM | HYDRA | 4 |
| | AN/SQS 505 | 7 | HM | Kortenaer | 8 |
| | DE 1191 | 5-7 | HM | Charles F. Adams | 2 |
| Norway | TSM 2633 (Spherion) | 6-8 | HM | Oslo | 3 |
| Portugal | DUBA 3A | 22.6-28.6 | HM | Cdt Joao Belo | 3 |
| | AN/SQS 510 | 4.3-8 | HM | Cdt Joao Belo | 3 |
| | | | HM | Vasco da Gama | 3 |
| Spain | AN/SQS 35 | 13 | VDS | Baleares | 5 |
| | AN/SQS 56 (DE 1160[#]) (DE 1164) | 6.7-8.4 | HM | Baleares | 5 |
| | | | | Descubierta | 6 |
| | | | | FFG 7 | 6 |
| Turkey | AN/SQS 26 | 3 | HM | Knox | 5 |
| | AN/SQS 56 (DE 1160[#]) (DE 1164) | 6.7-8.4 | HM | Barbaros | 4 |
| | | | | FFG7 | 7 |
| | | | | YAVUZ | 4 |
| | DUBA 25 | 8-10 | HM | Type A69 | 6 |
| UK | Type 2016 | 4.5-7.5 | HM | Invincible | 3 |
| | | | | Type 42 | 7 |
| | Type 2050 | 4.5-7.5 | HM | Type 22 | 5 |
| | | | | Type 23 | 16 |
| | | | | Type 42 | 11 |
| USA | AN/SQS 53 | 3 | HM | Spruance | 10 |
| | | | | Ticonderoga | 27 |
| | | | | Arleigh Burke I/II/IIIa | 38 |
| | AN/SQS 56 (DE 1160[#]) (DE 1164) | 6.7-8.4 | HM | FFG 7 | 33 |

[1]HM: hull-mounted; VDS: variable-depth sonar.
[2]Number of units is the total number in each country's navy, NOT the number of those units in the exercise.
*May actually be an acoustically passive, rather than active, sonar system; not clear from the references.
[#]The DE 1160 and DE 1164 systems are very similar to the SQS 56 sonar.

the Mediterranean Sea is atypical of those found at mid to low latitudes in other parts of the world's oceans, where the depth of the waveguide centre is several hundred metres.

The acoustic waveguide that appears to have been present in the other mass stranding events discussed here is of a different type than the SOFAR channel. It existed in the uppermost part of the water column, again corresponding to the depths where the acoustic sources were operating (8m and 6m for the AN/SQS 53C and 56 sonars, respectively, and 5-10m for the typical deployment depths of seismic air gun arrays). These waveguides at the surface, called surface ducts, are fairly common features throughout the world's oceans, particularly during the winter and spring months (Urick, 1983). They are formed by mixing of the near-surface waters by convection and by ocean surface wave activity generated by atmospheric winds. This mixing forms a surface layer with nearly constant temperature so that sound speed increases with depth in the layer solely due to an increase in pressure. For purely isothermal conditions, the sound speed gradient is expected to be 0.016m $s^{-1}$ $m^{-1}$ (Jensen *et al.*, 1994, p.25). A smaller positive sound speed gradient can occur due to very slight decreases in temperature with depth, as appears to have occurred during the March 2000 Bahamas event (Anon., 2001; Fromm and McEachern, 2000).

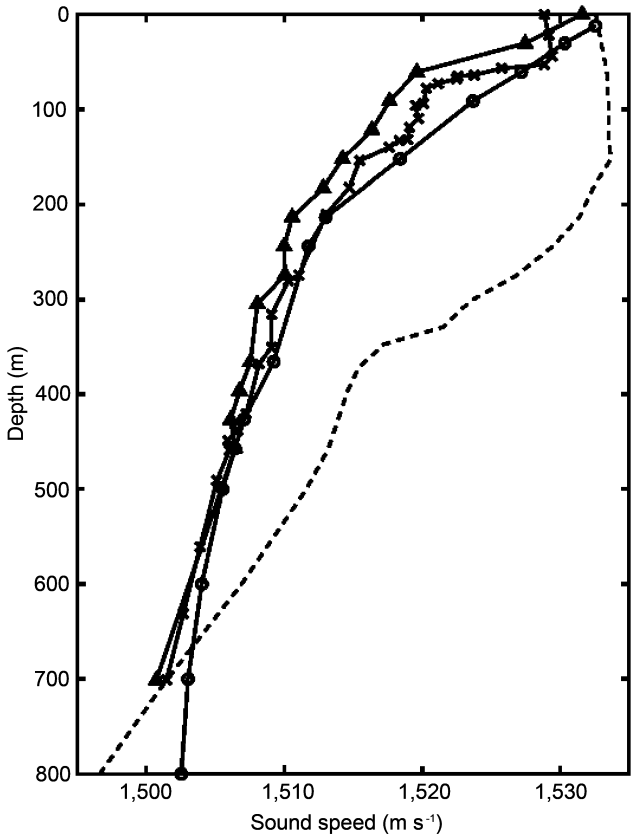


Fig. 1. Sound speed profiles derived from 3 XBTs collected in the vicinity of the Canary Islands around the time of the 2002 stranding event (plotted as circles, triangles and 'x's) along with the XBT-derived sound speed profile from the Bahamas 2000 event (dashed curve). An XBT measures temperature as a function of time after its deployment. The temperature data were converted into sound speed using an empirical equation of state for seawater and a salinity profile representative of the location of interest, typically extracted from an oceanographic database. An assumed descent rate for the XBT was used to derive depth. Deviations of the true descent rate from that assumed can lead to distortions in the derived sound speed profile, therefore, the surface duct depths of about 50m in the Canary Islands and about 150m in the Bahamas 2000 XBT are only approximations.

Fig. 1 shows the sound speed profiles derived from three expendable bathythermograph (XBT) profiles taken in the vicinity of the Canary Islands around the time of the 2002 naval exercise along with an XBT-derived sound speed profile from the Bahamas 2000 event (dashed curve). Two of the Canary Islands profiles show downward-refracting conditions near the surface (i.e. a steady decrease in sound speed with increasing depth), but one profile (denoted by 'x's) indicates the presence of a surface duct of about 50m thickness. The surface duct in the Bahama 2000 profile is about three times this thickness. This feature effectively traps mid to high frequency sound radiated by acoustic sources within the duct, such as surface ship sonars, so that the properties of the water column at greater depths and the ocean bottom are of secondary importance except at close range or close to land. At low frequencies, the sound is no longer effectively trapped by the duct because the acoustic wavelength (equal to the medium sound speed divided by the frequency) is too large in comparison to the duct thickness. The minimum frequency, $f_{min}$, in kilohertz, trapped by a surface duct of thickness $H$, in metres (Urick, 1983, p.151) is,

$$f_{\min} \simeq 176 / H^{3/2}$$

As an example, the minimum frequency for a 50m duct is 500Hz.

The physical processes of surface layer mixing that create and maintain surface ducts at mid and lower latitudes also tend to decrease the acoustic transmission efficiencies of these ducts. That is, the roughness of the ocean surface due to wave activity scatters sound out of the duct. Note that a weak sound speed gradient in the duct, as apparently existed in the Bahamas incident, can help reduce the scattering effects due to surface roughness by causing the sound field to interact at more grazing incidence with the surface. In addition, wave breaking injects bubbles into the water column that significantly scatter and absorb sound at mid-frequencies and above (i.e. above 1kHz). Without these mixing processes, the near-isothermal mixed layer conditions necessary for surface ducts are soon lost through

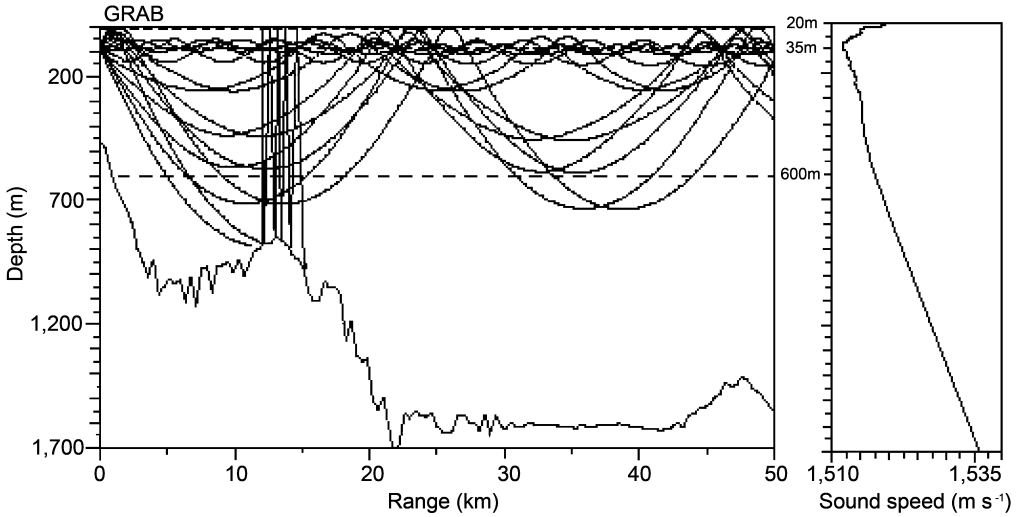


Fig. 2. Ray-trace for the sound field from the TVDS source at 85m depth in the 1996 Greek mass stranding event along with the sound speed profile. Rays were launched from the source at 0km range in the angular interval about the horizontal direction corresponding to the vertical beam pattern of the TVDS source (Table 1). Horizontal dashed lines are placed at 20, 85 and 600m depth in the left panel (fig. 8.2.1 of D'Amico and Verboom, 1998).

solar heating. In fact, the diurnal variability of surface ducts has been recognised for over a half century and is referred to as the 'afternoon effect' (Urick, 1983). These and other properties of surface ducts have been extensively studied due to their importance in surface ship tactical sonar performance (e.g. Schulkin, 1968; Baker, 1975; Urick, 1979; 1983; Hall, 1980).

Therefore, the most acoustically efficient surface duct conditions exist shortly after medium to strong winds (sufficient to cause wave breaking) have subsided and solar heating of the surface layer is minimised, e.g. by cloud cover or night. Since the pitching/rolling motion of a surface ship is reduced, calm sea conditions also help keep the main beam of hull-mounted sonar systems directed into the surface duct. In addition, the naturally-occurring background noise levels in the ocean (predominantly associated with ocean surface wave activity; Wenz, 1962) generally decrease under calm conditions so that the signal-to-noise ratio (SNR) of man-made signals correspondingly increases. Calm sea conditions with a pronounced surface duct prevailed in the New Providence Channel during the March, 2000 event (Anon., 2001; Fig. 1). Likewise, an anomalous weather pattern that led to the absence of trade winds existed during the 2002 Canary Islands event. In addition, the situation that resulted in the strandings appears to have occurred at night, since the initial discovery of the stranded animals occurred in the morning (Department of the Environment, 2002).

Enclosed basins may also present special conditions for the existence of surface ducts. Under open ocean conditions, white caps, which indicate the presence of bubbles, typically begin to occur when the wind speed exceeds 7-10kts i.e. 3-5m $s^{-1}$ (Wenz, 1962). This white-capping activity is modulated by open ocean swell (Phillips, 1977). In enclosed basins, where deep ocean swell activity is reduced by bathymetric/topographic blockage, the onset of white-capping may be suppressed.

A further environmental factor that plays a role in the efficiency of sound propagation at higher frequencies is the average water temperature. Sound absorption increases with decreasing temperature above 3kHz so that, whereas the received sound levels at 30km range at 3kHz are less than 1dB lower in waters at 4°C than in 24°C waters, they are 10dB lower at 8kHz and 15dB lower at 10kHz. A near-surface water temperature of 24°C is representative of the conditions in the Bahamas 2000 event (Anon., 2001; Fromm and McEachern, 2000). The temperature dependence of sound absorption is discussed later.

## PROPERTIES OF PROPAGATION

Several textbooks describe the properties of acoustic fields in detail (e.g. Brekhovskikh and Lysanov, 1991; Jensen *et al.*, 1994; Kinsler *et al.*, 1982; Medwin and Clay, 1998; Richardson *et al.*, 1995; Tolstoy and Clay, 1987; Urick, 1979; 1983). Only brief comments on one aspect of acoustics, that of sound propagation in waveguides, are provided here given its potential significance to the stranding events discussed in this paper.

An important aspect of the acoustic focusing effects of waveguides is the change in the rate of geometrical spreading after a certain transition range, $r_t$. In a waveguide, the decrease in sound pressure amplitude with increasing range due to geometrical spreading occurs at the rate of the inverse square root of the range ('cylindrical' spreading) after the transition range (because the sound field has now filled the waveguide), rather than decreasing inversely with the range itself ('spherical' spreading). Note that arrays of sources, properly oriented, can fill a waveguide with sound more effectively than individual sources, thereby decreasing geometrical spreading loss. The net result of the difference in geometrical spreading is that the acoustic energy in a duct (proportional to the square of the pressure amplitude, on average) decreases at a rate that is the range times smaller than in spherical spreading, at ranges greater than the transition range. An equivalent statement is that the transmission loss (TL) due to cylindrical spreading increases with the range, $r$ after the transition range, $r_t$, as

$$20\log\frac{r_t}{r_{ref}}+10\log_{10}\left(r/r_t\right)$$

where $r_t$ is the transition range, compared to:

$$20\log_{10}\left(r/r_{ref}\right)$$

for spherical spreading ($r_{ref}$ typically is 1m), so that the difference between the two in decibels after $r_t$ equals:

$$10\log_{10}\left(r/r_t\right)$$

Therefore, received sound fields in waveguides created by sources within them have significantly higher levels than otherwise at ranges greater than the transition range. The numerical modelling results presented later quantify this difference for some simple environments.

The waveguide boundaries are more important in determining the sound propagation characteristics than the interior of the waveguide itself. In shallow water (e.g. near the coast) and at low frequencies, a waveguide is often formed by reflection from the underside of the sea-surface and reflection from the ocean bottom. In these cases, the water depth and its spatial variation have a significant effect on the propagation properties. In addition, interaction with the bottom causes loss of energy from the sound field. This loss is due both to sound penetration into the bottom, which usually is much less efficient at transmitting acoustic energy than the ocean, and to scattering from bottom roughness. Broadband propagation in shallow water waveguides is also quite dispersive. Dispersion occurs when the speed at which energy is transferred down the waveguide, called the group speed, is a function of frequency. This frequency dependence causes the time spreading of a broadband pulse to increase with increasing propagation distance. In shallow water, the energy at higher frequencies is transferred at higher group speeds than at lower frequencies (that is, until the frequency becomes so low that most of the energy is effectively travelling within the ocean bottom). Therefore, the received waveform in shallow water from a source such as an air gun or an explosion will not be a pulse. Instead, it generally will begin with the highest frequencies and evolve to lower frequencies with increasing time. The total duration of the arriving signal increases with increasing range and the received signal duration can be used to estimate the range of the source.

A waveguide boundary also can be formed by refraction due to the increase in water sound speed with increasing distance from the central axis of the waveguide. Sound propagating in acoustic waveguides formed by refraction in the water column usually attenuates at a much lower rate than in shallow-water-type waveguides because it is isolated from interaction with the ocean boundaries. The effect is particularly pronounced when isolated from the sound-attenuating ocean bottom. In fact, ocean acoustic

waveguides formed by refraction within the water column are some of the most efficient waveguides for energy transmission found in nature. The frequency dispersion of broadband pulses in these types of waveguides can be negligible. Group speeds can either increase or decrease with frequency, but typically at significantly lower rates than in shallow water. The reason is that, from a ray theory point of view, the increase in propagation distance of more steeply propagating rays is compensated for (partially to fully depending upon the sound speed gradients) by the increase in medium sound speeds with increasing vertical distance from the waveguide axis (depth of minimum sound speed). In effect, pulses tend to remain as pulses during propagation. One consequence is that rapid signal rise times are not degraded appreciably by frequency dispersion during propagation, but change only as a result of frequency-dependent attenuation mechanisms.

## PREDICTION OF SOUND FIELD PROPERTIES

The issues that need to be addressed to accurately predict the properties of the underwater sound field during mass stranding events are: (1) the transmission characteristics of the sources (e.g. signal types, levels, frequency content, duty cycle, directionality, etc.) and times of transmission and locations of the sources over the course of the event; (2) the important environmental phenomena that need to be included in the modelling; (3) the capability of the propagation codes to accurately model the important environmental phenomena (i.e. how well do the models capture the relevant physics); and (4) the availability and quality of the environmental information required as input to the propagation models. Each of these topics will be discussed in turn.

Regarding the first issue, the properties of the TVDS source and the nominal characteristics of the hull-mounted sonar systems are well known, as described earlier (although changes in hull-mounted sonar performance over time due to aging and use are not accounted for since frequent system calibrations are not performed; Anon., 2001). However, the actual output levels and directionality of seismic air-gun arrays at higher frequencies are presently active areas of investigation (e.g. Diebold *et al.*, 2003). Information on source location over time typically is recorded in a ship's log(s), although that information may not be openly available.

The environmental property of greatest relevance in these events is probably the spatial dependence of the ocean sound speed; primarily on depth, but also on range and azimuth. This sound speed information determines the existence and spatial extent of any ducts or sound channels and dictates the overall propagation characteristics. A second important environmental property is the intrinsic sound absorption of the ocean. At the frequencies of interest here, this is due primarily to endothermic reactions associated with magnesium sulphate and boric acid (Fisher and Simmons, 1977). It increases approximately at the rate of the square of the frequency and so becomes increasingly important with increasing frequency in limiting the spatial extent of propagation (see later). Note that wind-generated ocean ambient noise in the mid to high frequency band also decreases approximately at the rate of the square of the frequency (Wenz, 1962), so the received signal-to-noise ratios from sources with frequency-independent source levels also are roughly frequency independent. For sound fields that interact with the ocean surface as in surface duct propagation, the roughness of the sea-surface and the near-surface bubble content of the water column are important features. For waveguides formed by refraction within the water column, the temporal and spatial variability of the water column in the refraction region, for example due to internal wave activity, may play an important role. Significant factors for sound fields that interact with the ocean bottom (including those in shallow water and at short range to the source unless the directional characteristics of the source reduce bottom interaction as with the TVDS and hull-mounted sonars) are the bathymetry, interface roughness and sub-bottom geoacoustic properties.

Other phenomena that pertain to propagation at mid frequencies such as the presence of fish schools, precipitation, and nonlinear internal waves (e.g. solitons), may also be significant in certain situations.

Once the relevant environmental phenomena have been identified, numerical propagation codes that incorporate the physics of sound field interactions with these phenomena must be used in the modelling effort. The physics of sound propagation is based upon the laws of conservation of mass, linear momentum and energy. The equations expressing these laws are typically combined to obtain the acoustic wave equation, a second order partial differential equation that expresses the relationship between changes in space and time of acoustic pressure. Equations can be derived for other acoustic field variables, e.g. acoustic particle velocity, acoustic density and vector acoustic intensity, but acoustic pressure is almost always the quantity of interest. One of the prominent achievements of the acoustics community over the past few decades has been the development of more accurate numerical modelling techniques for acoustic propagation in increasingly complex environments.

Numerical models for ocean sound propagation mainly fall into one of four categories, ray-based codes, normal mode codes, those based on the parabolic equation (PE) approximation to the wave (elliptical) equation and wave number integration codes (Jensen *et al.*, 1994). Propagation codes of each type, as well as others are freely available at the Ocean Acoustics Library website *http://oalib.saic.com*. Methods such as finite element and finite difference techniques can be applied in highly complex and variable environments, but typically require high computing power and long run times. In any case, each of these modelling approaches is based on certain approximations and assumptions in order to calculate the fields in a computationally efficient way. As a result, a given approach is applicable only for a certain realm of propagation conditions. In addition, most codes are not numerical solutions to the acoustic wave equation itself, but rather its frequency-domain analogue (the Helmholtz equation) and so must be run several times to model broadband propagation. Results from an advanced ray-based code (Gaussian Ray Bundle, GRAB; Weinberg and Keenan, 1996) are reported by D'Amico *et al.* (1998). Codes based on all four approaches were used to predict the received fields in the Bahamas, 2000 incident for a small subset of environments (Fromm and McEachern, 2000), although reported results for a wide range of environmental conditions were obtained using a PE-based code (Collins, 1995). Recent enhancements to the PE approach incorporate many of the environmental complexities found in surface duct propagation (Norton *et al.*, 1998).

Accurate predictions of the acoustic field properties require not only the inclusion of the relevant physics in the numerical model, but also availability of accurate information on the environmental inputs. In most cases, collection and/or availability of measured environmental

data for a stranding event is very limited. In some instances, a few *in situ* profiles of water temperature may have been collected to derive the dependence of water sound speed on depth. The spatial dependence of the sound speed profiles throughout the area of interest typically must be inferred from historical databases, or possibly from fine-scale oceanographic models (e.g. Fox, 1996). Historical databases also provide information on the pH of the water column, which provides a measure of the amount of boric acid present and is required for accurate estimates of intrinsic sound absorption. At the least, approximate absorption estimates can be obtained from *in situ* measurements of water temperature alone (see later). Sea-surface roughness, particularly important in surface duct propagation situations, can be estimated using a model of the ocean surface wave spectrum (e.g. Pierson and Moskowitz, 1964) if the wind speed is known or possibly from visual observations. The bubble content and distribution in the near-surface layer and the degree of internal wave activity are only estimates. In contrast, large-scale ocean bathymetric information is readily available for situations in which bottom interaction is important (Sandwell *et al.*, 1998). However, the geoacoustic properties of the bottom and its roughness must often be inferred from the geological setting. In any case, uncertainty in the environmental inputs is probably the source of greatest error in predicting sound fields. Lack of knowledge of the animals' locations over time is an even greater source of error if an attempt is made to use the acoustic modelling results to estimate the animals' maximum received levels and 'unweighted sound exposure' (defined as the integral of pressure squared over time; American National Standards Institute (ANSI, 1994)).

An example of a numerical modelling output for one of these events is presented in Fig. 2. This ray tracing result, from the SACLANTCEN report of the 1996 Greek stranding event (fig. 8.2.1 of D'Amico and Verboom, 1998), was calculated using the GRAB propagation code (Weinberg and Keenan, 1996). The input sound speed profile and ocean bathymetry are plotted in the right panel. The profile shows a sound channel with a sound speed minimum (axis) at 85m, corresponding to the depth of the TVDS source. The main beam of the source was directed horizontally along the sound channel axis. The ray traces in the left panel provide a picture of the paths of acoustic energy flow as a function of range and depth. They show that two types of waveguides dictated the propagation characteristics. One waveguide, spanning the upper 800m or so, was formed by reflection from the ocean surface and refraction in the mid water column. The second was formed purely by refraction, which confines the acoustic energy to a relatively narrow depth interval centred at 85m at all ranges. The received sound levels at a given range are highest (by around 10dB; D'Amico and Verboom, 1998) within this depth interval (see below). The vertical directionality of the source minimised the interaction of the sound field with the ocean bottom at close range (Fig. 2). Significant interaction did not occur until the 10-15km range and the resulting reflection and scattering of the field to shallower depths likely did not contribute significantly to the received levels.

Several additional examples of numerical modelling results specific to the 1996 Greek event and the Bahamas 2000 event can be found in D'Amico *et al.* (1998) and Fromm and McEachern (2000) respectively. An overall comparison of the results for the two events shows that the received levels at 3kHz at a given range differ by about 10dB due to the difference in the sonar source levels in this frequency band (Table 1). Some of the important aspects of waveguide propagation, particularly propagation in surface ducts, are presented below.

## GENERAL MODELLING RESULTS

### Simple numerical modelling

The importance of waveguides in underwater sound propagation, as discussed previously, can be illustrated with some simple examples. Two cases have been considered, one that is representative of the environmental conditions in the 1996 Greek event and one that illustrates the focusing effects of surface ducts. In both cases, the environmental properties are independent of range and azimuth, including the water depth which was fixed at 1.5km. Also, the source frequency was 3kHz in both cases. Calculations were performed using the GRAB ray tracing code that uses a Gaussian ray bundle approach for deriving the sound field amplitudes (Weinberg and Keenan, 1996).

Fig. 3 shows the ray tracing results over depth and range out to 30km for a sound speed profile representative of those collected in the 1996 Greek event (the profile in the left panels is nearly identical to that in Fig. 2). The source is placed at 8m depth for the upper right panel whereas it is at 85m in the lower panel. The source depths are indicated by the horizontal dotted lines in the sound speed profile plots. For an 8m source in this environment, a 'shadow zone' – i.e. a region that contains no rays and thus has very low sound levels – exists in a semi-circular region that extends approximately 1-26km in range. This shadow zone is partly filled by energy that reflects off the bottom (rays requiring more than one bottom reflection to reach the 30km range have been suppressed in this plot for clarity), but bottom interaction significantly lowers the sound levels received by shallow receivers. In contrast, the sound field created by a source at 85m depth, corresponding to the depth of the waveguide axis, fills in this shadow zone at depths below the source to a large extent. Sound is also focused in a depth interval centred at 85m at all ranges.

These observations from the ray-trace plots are further illustrated in the corresponding transmission loss versus range plots at 3kHz presented in Fig. 4. These plots were obtained by incoherently summing the individual ray energy to obtain the total field at a given range, equivalent to incoherently averaging the field over small range intervals centred on the range. The solid curve in each panel on the right is for a source at 8m and the dotted curves are for a source at 85m. The receiver depth is 8m in the upper right panel and 85m in the lower right panel. The straight portion of the two curves in the upper right panel and the solid curve in the lower panel (i.e. for an 8m source/8m receiver, 8m source/85m receiver and 85m source/8m receiver), extending from a few kilometres to 25-26km represent the shadow zones for these source/receiver combinations. The received levels in these regions are determined by bottom-reflected energy and therefore show large transmission loss. Over a range interval of 25-30km, the change with depth in the sound speed profile at depths greater than 100m causes a focusing of the refracted rays and the received levels to increase by 20dB or so. This focusing effect clearly illustrates the impact of the sound speed profile on the character of ocean-borne sound fields.

An even more dramatic focusing effect is shown by the dotted curve in the lower right panel of Fig. 4, corresponding to the transmission loss versus range for a receiver at the waveguide axis depth of 85m due to a source at this same depth. The sound field levels are 20dB greater

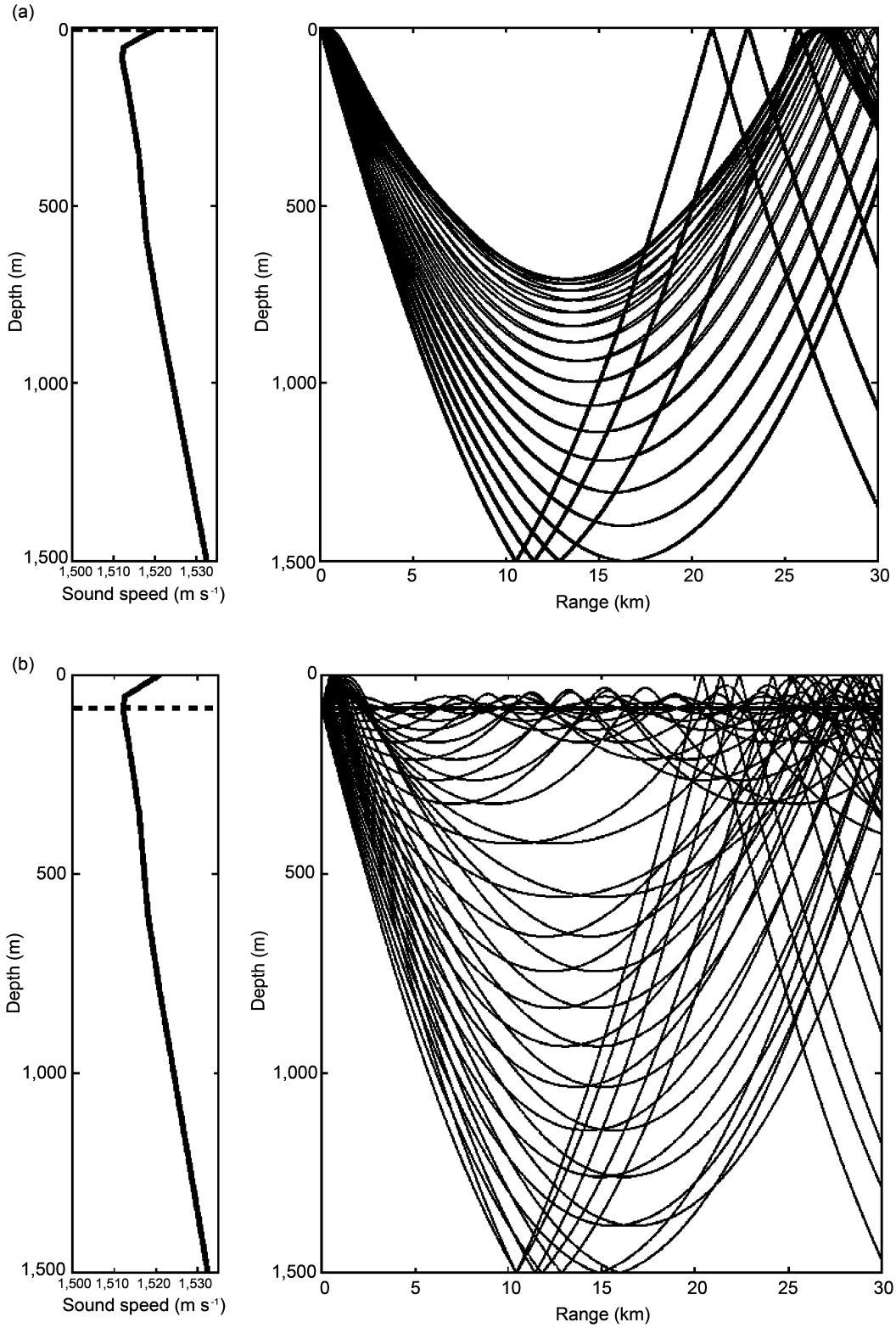


Fig. 3. Ray-trace in range and depth for a Mediterranean-like sound-speed profile (left) for a source depth of 8m (upper plot) and 85m (lower plot).

than the other source/receiver combinations at almost all ranges greater than the 1-2km transition range because of the focusing effects of the waveguide.

In the next example, presented in Figs 5 and 6, the source depth remains fixed at 8m. However, the sound speed profile in the uppermost 100m is modified from downward-refracting conditions (the sound speed steadily decreases with increasing depth) to surface ducting conditions (the two profiles in the leftmost panels). The corresponding ray-tracing plots show how the ray paths are altered by the surface duct, causing a focusing of sound in the near-surface waters. These effects are quantified in the transmission loss as a function of range plots in Fig. 6, where the levels received at 8m depth in the presence of a surface duct (the

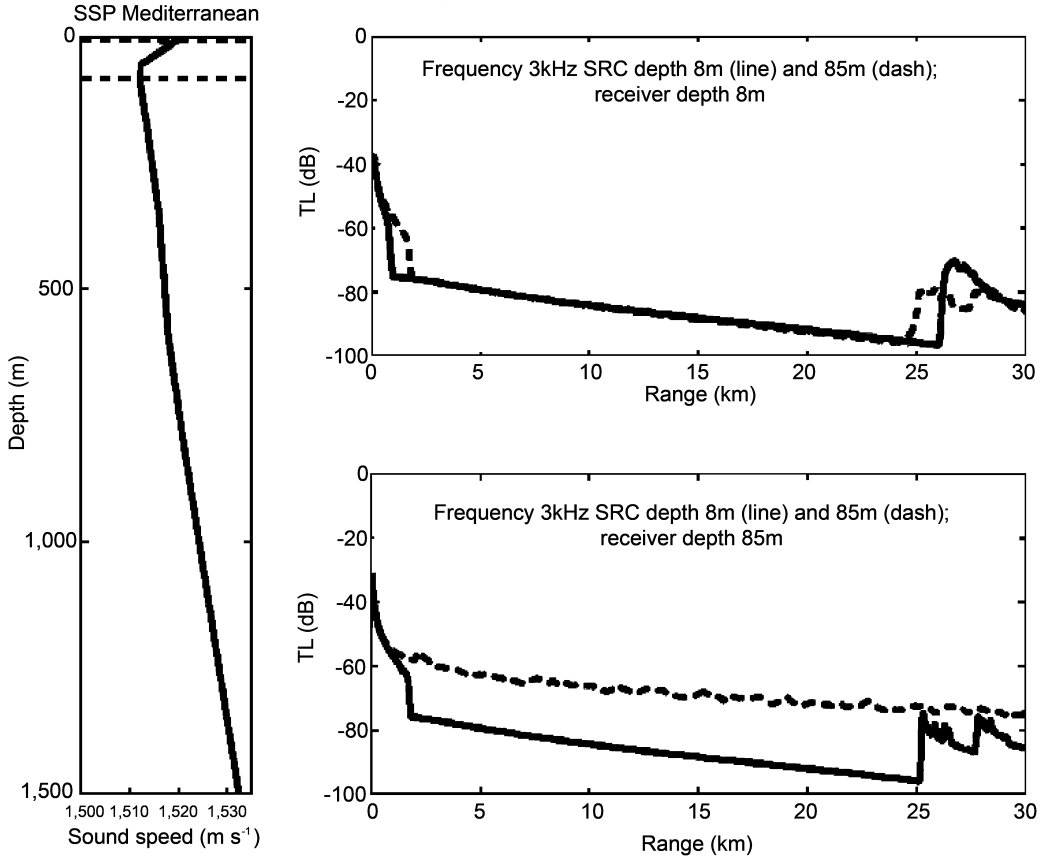


Fig. 4. TL as a function of range for a Mediterranean-like sound speed profile (left) with source depths of 8m (solid lines) and 85m (dashed lines) and receiver depths of 8m (upper right) and 85m (lower right). The estimated received levels as a function of range for a specific source can be easily determined by adding the source's source level from Table 1 to the TL values in the plots. For example, at 5km in the upper plot where the TL is 80dB, the estimated received level for the TVDS mid-frequency source is 146dB re: 1μPa (= 226dB – 80dB).

solid curve in the upper right panel) are 15-20dB greater than otherwise past the 1km transition range. The reason for choosing a receiver depth of 300m for comparison was so that it was significantly deeper than the base of the duct.

The main conclusion to draw from these examples is that the depth-dependence of the sound speed profile can have a dramatic effect on the properties of an underwater sound field. In particular, the sound levels inside an acoustic waveguide created by a source within the waveguide are significantly greater at almost all ranges greater than the transition range than when a waveguide does not exist or when either the source or receiver is not within the waveguide.

**A semi-empirical model of surface duct propagation**

The previous examples are simplified representations of naturally-occurring propagation conditions. For example, no rough surface scattering, interaction with near-surface bubbles, or horizontal variability of the environment was included. Because of the importance of surface ducts in hull-mounted sonar system performance, extensive measurements of surface duct propagation have been made throughout the world's oceans (Urick, 1979; Urick, 1983). Before the advent of modern computers, the measurements were fitted with simple semi-empirical equations to give a prediction capability. These equations account for transmission loss due to geometrical spreading, intrinsic absorption and duct 'leakage'. This latter term includes the effects of all physical processes not taken into account by the other two terms. These equations provide a simple, data-based method of evaluating the changes in propagation conditions due to changes in environmental properties. The semi-empirical surface duct propagation model discussed in this subsection is that given in Baker (1975). In the Baker model, the transmission loss, TL, in decibels is given by:

for short ranges, $r < 0.204\sqrt{H}$

$$\mathrm{TL} = 20\log_{10}(r) + 60.8 + (A+B)r$$

for long ranges, $r > 0.204\sqrt{H}$

$$\mathrm{TL} = 10\log_{10}(r) + 5\log_{10}(H) + 53.9 + (A+B)r$$

In truth, the transition between short and long range in Baker (1975) is given as $\sqrt{0.122H}$, but the value above is used so that the transmission losses given by the two expressions are equal at the transition range. Units for the quantities in these expressions are; $r$ in units of km, the surface duct thickness, $H$, in metres, and the attenuation coefficients, $A$ and $B$, with units of dB km$^{-1}$. The constants 60.8 and 53.9 provide the necessary corrections so that transmission loss in dB referenced to 1m is obtained. The terms involving the logarithm express the loss due to geometric spreading and are derived from the conservation of acoustic energy. The coefficient $A$ is due to sound absorption in the water column. In the Baker model, it is a function of frequency

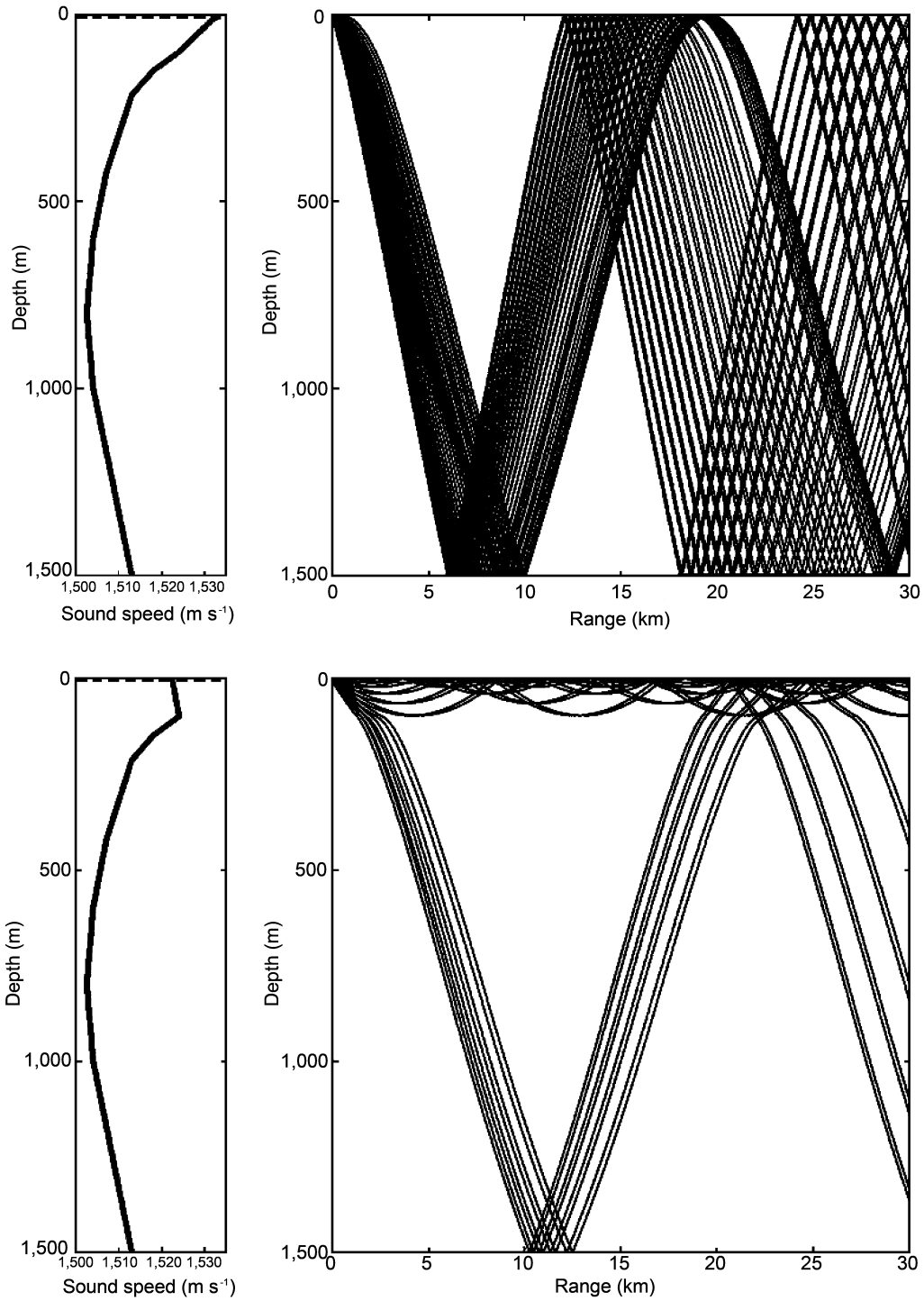


Fig. 5. Ray-trace in range and depth for an omni-directional point source at 8m depth in two eastern Atlantic-like environments that are identical except in the uppermost 100m (left). One has a monotonically decreasing sound speed profile with increasing depth (upper plot) whereas the other one has a 100m thick surface duct (lower plot).

and water temperature only. The expression for *A* (obtained from work by H.R. Hall at the Naval Undersea Warfare Centre) is:

$$A = \frac{1}{0.9144}\left[\frac{1.776 f^{1.5}}{32.768 + f^3} + \frac{1}{1 + 32.768/f^3}\left(\frac{0.65053 f^2 f_T}{f^2 + f_T^2} + \frac{0.026847 f^2}{f_T}\right)\right] dB\ km^{-1}$$

where the frequency, $f$, is in kHz, $f_r = 21.9 \times 10^{[(6T + 118)/(T + 273)]}$, and $T$ is the water temperature in °C.

The duct leakage coefficient, $B$, is a function of duct thickness and sea-state as well as frequency and temperature, i.e.:

$$B = \frac{29.1 f}{\sqrt{\left[\left(1452 + 3.5T\right) H\right]}} \left(1.4\right)^{SS}\ dB\ km^{-1}$$

where SS is the sea-state (see Wenz, 1962 for descriptions of sea-states).

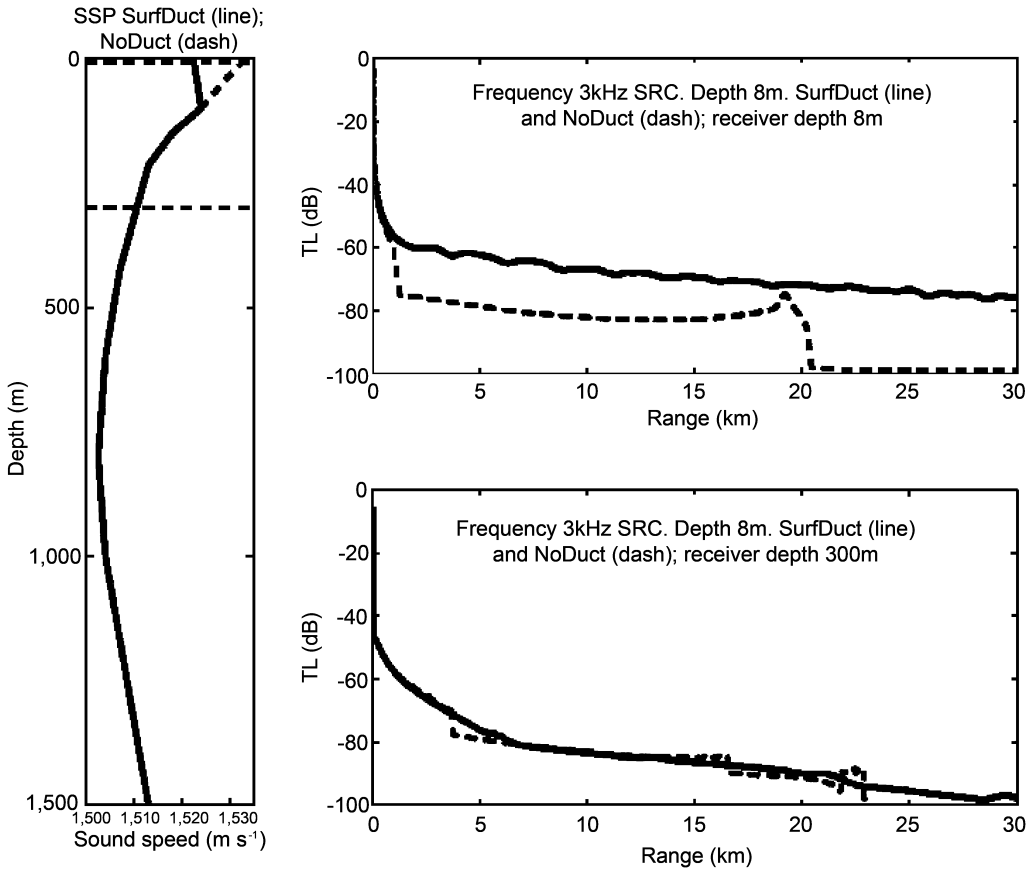


Fig. 6. TL as a function of range for two eastern Atlantic-like sound speed profiles (left) with a source depth of 8m and receiver depths of 8m (upper right) and 300m (lower right). The dashed curves are for a profile with a monotonically decreasing sound speed with increasing depth over the uppermost 100m and the solid curves are for a profile with a 100m thick surface duct. Refer to the caption for Fig. 4 to determine how to convert these TL values versus range into estimated received levels for a given source.

The Baker model was obtained by curve-fitting to a total of 438 open-ocean measurements where all the free parameters in the fit were contained in the coefficient B. The mean errors of the fit were ± 2dB with a standard deviation of 7dB. The result is strictly valid for the range of environmental conditions and experimental geometries in which the data were collected. These were:

Environmental:

| | |
|---|---|
| duct depth | 24 – 67m |
| water temperature | 15 – 25°C |
| sea-state | 2 to 5 |

Geometry:

| | |
|---|---|
| source, receiver depths | 9.1 – 18.3m |
| source/receiver range | 1 – 31km |
| frequency | 3.25 – 7.5kHz |

The near-surface water temperatures in the Bahamas and Canary Islands events are at the upper end of the interval of temperatures in Baker's data sets. Also, although the surface ship sonar depths were slightly less than the source depths in Baker's data sets and some of the transmitted frequencies may be slightly outside the 3.25-7.5kHz band, the deviations are not large and the Baker model predictions should provide representative results for these events.

The attenuation coefficients *A* and *B* in the Baker model contain all of the frequency dependence of the transmission loss of acoustic fields in surface ducts. Whereas *A* is a complicated function of frequency, the expression for *B* shows that duct leakage increases in a simple linear way with increasing frequency. The expressions for these coefficients also quantify the effects of changes in environmental conditions on transmission loss. For example, the value of the sea-state appears as a power law exponent in the expression for *B* so that for each step increase in sea-state, the duct leakage increases by a factor of 1.4. In addition, B is inversely proportional to the square root of the duct depth. To illustrate the effects of changes in these properties, Fig. 7 provides a plot of the duct leakage coefficient in units of dB km$^{-1}$ for duct thicknesses of 60m and 100m at sea-states 2, 3, 4 and 5. The plot shows that a doubling of the duct thickness has the same effect on *B* as a decrease by one in the sea-state (note that the constant of 1.4 in the expression for *B* approximately equals $\sqrt{2}$. Similarly, Fig. 8 provides plots of *A* (dotted curves), *B* (dashed curves) and the sum of the two (solid curves) as a function of frequency for the three water temperatures of 4°C, 15°C and 24°C. The duct thickness and sea-state are fixed at 60m and sea-state 2. Although duct leakage is only very weakly dependent upon water temperature, intrinsic absorption decreases with increasing temperature at frequencies above 3kHz. At 10kHz, the coefficient decreases from about 1dB km$^{-1}$ at 4°C to 0.5dB km$^{-1}$ at 24°C. Therefore, the 10kHz absorption loss at 30km decreases from 30dB to 15dB due to this 20°C increase in water temperature. Clearly warmer surface waters provide more favourable propagation conditions at the higher frequencies. Note that almost all of the sonar systems in Table 2 operate at these higher frequencies. An interesting question is whether or not lower absorption at higher temperatures is in any way related to

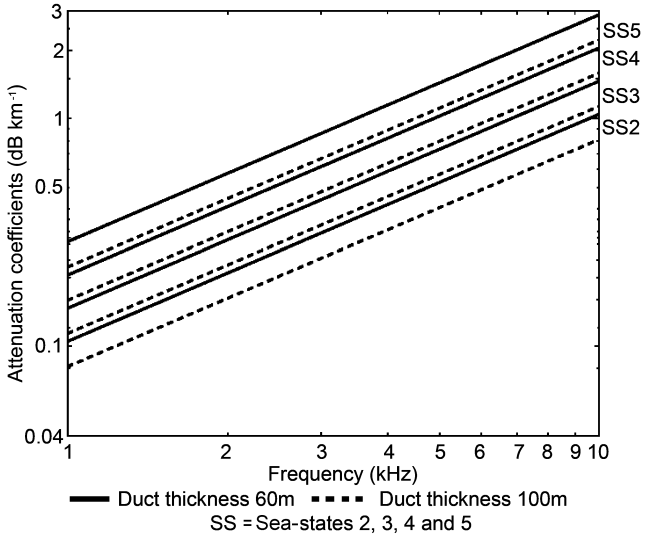


Fig. 7. Duct 'leakage' attenuation coefficients from the Baker model for duct thicknesses of 60m and 100m for four different sea-states.

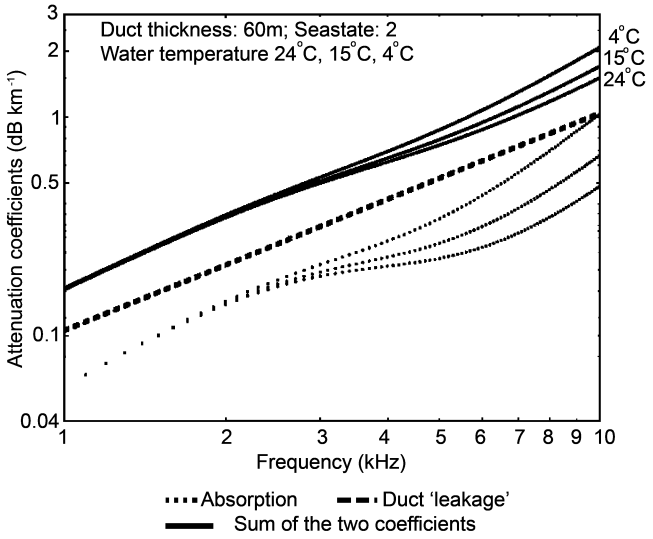


Fig. 8. Effect of changes in average water temperature on the two attenuation coefficients and their sum in the Baker model.

the observation that the number of animals involved in historical Canary Islands stranding events is greatest in the autumn, as reported on the Department of the Environment, Government of the Canary Islands website (2002).

Fig. 7 shows that thicker ducts have less leakage loss than shallower ducts. However, because of the difference in the range where the transition from spherical to cylindrical spreading occurs, thicker ducts also have greater geometrical spreading loss. The difference in TL for two ducts of thicknesses $H_2$ and $H_1$ (with all other conditions remaining the same) is:

$$\mathrm{TL}(H_2) - \mathrm{TL}(H_1) = 5\log_{10}\left(\frac{H_2}{H_1}\right) - \beta\left(\frac{1}{\sqrt{H_1}} - \frac{1}{\sqrt{H_2}}\right) r$$

where:

$$\beta \equiv \frac{29.1 f}{\sqrt{\left[\left(1452 + 3.5T\right)\right]}} \left(1.4\right)^{SS}$$

Since the second term on the right hand side depends on range whereas the first does not, the transmission loss for a thicker duct changes from being greater than to being less than that of a shallower duct at some crossover range. As an illustration, Fig. 9 shows the TL versus range curves predicted from the Baker model for two duct depths of 60m and 100m at a frequency of 3kHz, a water temperature of 24°C and a sea-state of 2. The crossover range is 16km, as can be determined by setting the TL difference above to zero and solving for range. However, the difference between the two curves is not significant. Therefore, the dependence of the received sound levels on duct thickness is probably negligible. This result holds for frequencies that are appreciably greater than the low frequency cut-off for the duct.

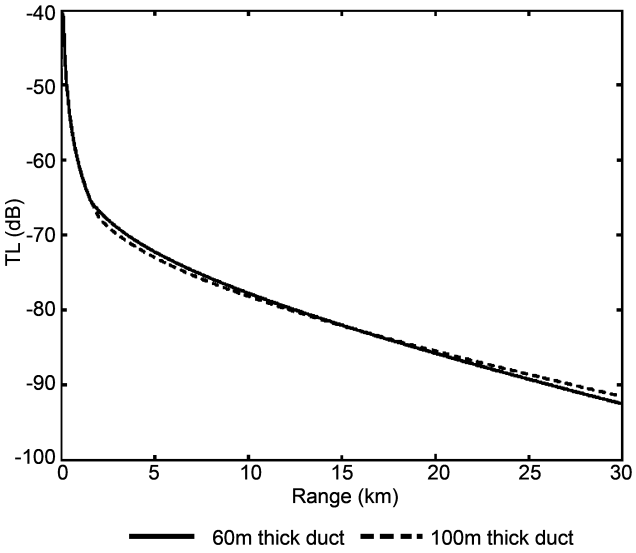


Fig. 9. Transmission loss as a function of range for two different duct thicknesses as predicted by the Baker model. The solid curve is for a duct thickness of 60m and the dashed curve for 100m. Sound frequency 3kHz, water temperature 24°C and sea-state 2.

**Calculation of unweighted sound exposure**

Sound exposure, SoE, defined as the integral of acoustic pressure, *p*, squared over time (ANSI, 1994), may be an important measure of a sound field's potential to cause temporary threshold shift (National Research Council, 2003). This quantity can be calculated in a straightforward way using a model for the transmission loss (e.g. the Baker model), knowledge of the source transmission properties and its motion and a model of the receiver motion.

The sound exposure for a single pulse of duration $T_s$, is defined as:

$$\mathrm{SoE(1\ pulse)} = 10\log_{10}\left[\int_0^{T_s} p^2(t)dt\right]$$

$$= 10\log_{10}[T_s] + 10\log_{10}\left[\frac{1}{T_s}\int_0^{T_s} p^2(t)dt\right]$$

$$= 10\log_{10}[T_s] + \mathrm{RL}$$

The received level, RL, from the sonar equation (Urick, 1983) is determined by the difference between the source level, SL, and transmission loss as a function of range, TL(*r*), so that:

$$\mathrm{SoE(1\ pulse)} = \mathrm{SL} - \mathrm{TL}(r) + 10\log_{10}[T_s]$$

The root mean square (rms) source levels for the sonar systems of interest are listed in the second row of Table 2, along with the pulse durations in the third row. The total sound exposure due to $N$ pulses where the source/receiver range changes from one pulse to the next is:

$$\mathrm{SoE(total)} = 10\log_{10}[T_s] + 10\log_{10}\left[\sum_{i=1}^{N} 10^{\frac{\mathrm{SL\text{-}TL}(r_i)}{10}}\right]$$

The values of $r_i$ in this expression can be obtained from knowledge of the source (ship) tracks and a model of the receiver motion. For example, assume that the source and the receiver travel at constant horizontal velocities with components of relative speed between them of $v_x$ and $v_y$ in the east/west and north/south directions, respectively. At the time of the first pulse, the initial source/receiver distances in the east/west and north/south directions are $d_x$ and $d_y$ and given that the interpulse time, $\tau$ (given on the fourth row of Table 1) is constant, then $t = (i-1)\tau$ and the range between source and receiver at the time of the $i$th pulse is simply:

$$r_i = \sqrt{\left(d_x + v_x(i-1)\tau\right)^2 + \left(d_y + v_y(i-1)\tau\right)^2}$$

In the following example, the environmental properties are those of a duct 100m thick, a water temperature of 24°C and a sea-state of 2, similar to the conditions preceding the Bahamas, 2000 event. Also, the frequency of the source is 3kHz and its signals have an interpulse time, pulse duration and source level equivalent to those listed in Table 1 for the AN/SQS 53C sonar (i.e. 24s, 2s and 235dB re: 1μPa at 1m, respectively). Only pulses with a received level above 160dB re: 1μPa were included in the calculation of the total sound exposure. The motions of the source and receiver were assumed to be such that their range was determined only by an initial range and a constant relative speed. Results for various combinations of starting source/receiver ranges and relative speeds are presented in Figs 10 and 11. The number of pulses that were received above the 160dB re: 1μPa threshold is presented in Fig. 10 and the resulting total sound exposure is shown in Fig. 11. Both quantities are plotted as a function of the relative speed between the source and receiver for positive values from 1-10m $s^{-1}$ in 1m $s^{-1}$ increments (positive relative speeds indicate that the source/receiver range monotonically increases with time). Each figure contains six curves pertaining to six starting source/receiver distances of 1km (uppermost curve in each figure) to 6km (lowermost curve) in 1km increments. The number of received pulses above the threshold (Fig. 10) shows a dramatic rise as the relative speed decreases below a few metres per second. A small relative speed occurs, for example, when the source and receiver tracks are co-linear and the receiver is ahead of the source and travelling at a slightly greater speed. The total sound exposure (Fig. 11) displays the corresponding change in values with the most rapid changes (slopes of the curves) occurring for changes in small relative speeds. The sound exposure values increase by nearly 10dB for a 10-fold decrease in relative speed from 10-1m $s^{-1}$ at all starting ranges. The effect of decreasing starting range is even greater, with a 15dB increase from 6-1km at all relative speeds. This sensitivity is indicative of the importance of the contributions of the pulses at the closest ranges.

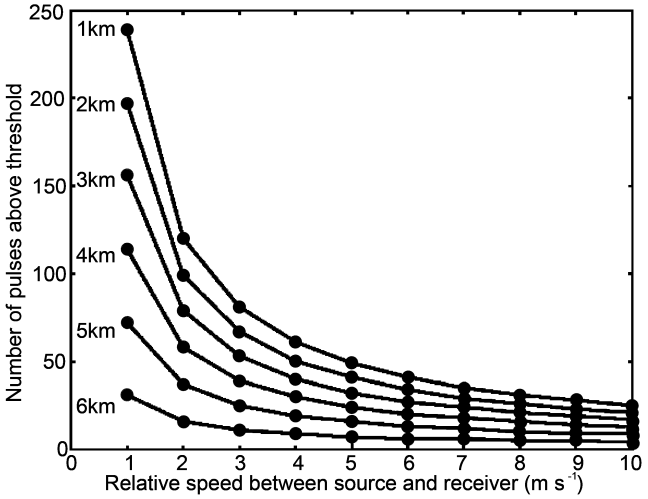


Fig. 10. Number of pulses with a received level above 160dB re: 1 μPa as a function of the assumed relative speed between the source and receiver for 6 starting source/receiver distances of 1-6km in 1km increments.

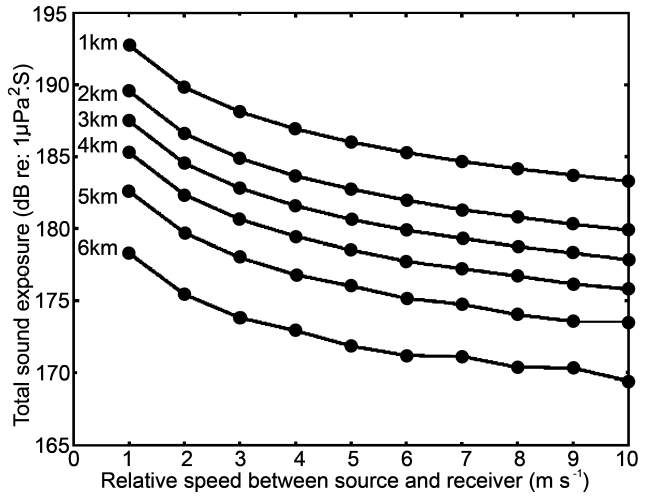


Fig. 11. Total unweighted sound exposure from pulses with received levels above 160dB re: 1μPa as a function of the assumed relative speed between the source and receiver for 6 starting source/receiver distances of 1-6km in 1km increments.

## CONCLUSIONS

The acoustic signals transmitted by the sonar systems during these stranding events and seismic air gun arrays have several features in common. The temporal character of each type of signal is a periodic sequence of transient pulses where the time interval between the pulses is on the order of tens of seconds (15-60s). The individual sonar pulses have a time duration of order a few seconds (1-4s) and contain similar types of waveforms (frequency-modulated 'chirps' and continuous-wave 'pings'), whereas a seismic air gun pulse is a short-duration (tens of milliseconds) impulse. In the frequency domain, all sources generate appreciable energy in the mid-frequency (1-10kHz) band (although the radiated spectral levels of seismic air guns in the mid-frequency band is a topic of investigation at present), with TVDS sources and air-gun arrays also generating significant amounts of lower frequency energy. The systems creating the sounds were all designed as source arrays to focus acoustic energy in a specific direction. Arrays of sources also allow the equivalent far-field source level to be much

greater than the water column's cavitation limit, which is about 230dB re: 1μPa at the depth of the hull-mounted sonar systems (Urick, 1983). All except the source in the 1996 Greek event were deployed at depths less than 10m. Finally, all sources moved at speeds of 5kts (2.6m $s^{-1}$) or more during operation.

The environmental settings for all cases was relatively deep water (1km or more) located close to land. Proximity to land is a requisite feature for strandings to occur. It is uncertain whether the environment accentuated the effects of the sounds through reflection and reverberation from the bathymetry. Very close to land, the shoaling bathymetry can focus the sound by a process called upslope conversion. In the cases involving sonar, the horizontal orientation of the source beams helped to minimise bottom interactions. These environmental settings may simply be the preferred habitats for beaked whales. In any case, most, if not all, water column conditions supported ducted waveguide propagation where at least one boundary of the waveguide (the lower one) was formed by refraction in the water column. In most, if not all, cases, the sound source(s) was located within the waveguide.

Sound propagation in acoustic waveguides formed by refraction in the water column has four features of potential significance to the events discussed here. (1) The sound radiated by sources within the waveguide is focused after a certain transition range so that geometrical spreading then occurs at the rate of cylindrical spreading, rather than the more rapidly decreasing spherical spreading. (2) The attenuation of the sound field with increasing range is minimised due to isolation from interaction with the ocean boundaries, particularly with the ocean bottom, which tends to scatter and absorb sound. In fact, ocean acoustic waveguides formed by refraction are some of the most efficient waveguides for energy transmission found in nature. For those events involving surface duct conditions, the weather conditions were calm, thereby decreasing the roughness of the sea-surface and the near-surface bubble content and increasing sound propagation efficiency of the duct. These conditions can also cause an overall decrease in the sound levels for receivers below the duct. Under calm conditions, the decrease in the pitching and rolling of the surface ships helps keep the main beams of their hull-mounted sonars focused within the duct and the decrease in wind-generated ambient noise levels results in an increase in the SNR of the transmitted signals. The average water temperature during the stranding event was relatively warm, thereby decreasing intrinsic absorption at frequencies above 3kHz. (3) The spatial gradients of the sound field amplitude with depth in the water column may be significant in the refractive boundary region. (4) The frequency dispersion of broadband pulses usually is minimal so pulses tend to remain as pulses and signal rise times do not increase appreciably during propagation.

The ability to predict the acoustic propagation characteristics during a given event is limited by the lack of knowledge of the environmental inputs, not by an inability to incorporate the relevant physics (once identified from the environmental conditions) into the numerical models. Unavailability of information on the location of source(s) with time also is a limiting factor in some cases.

Simple numerical models illustrate the focusing effects of waveguides. They show that 20dB increases in received sound levels can occur over extended range intervals after the transition range (typically 1km in extent in the examples presented here) when waveguide propagation conditions exist and both source and receiver are located in the waveguide. Data-based, semi-empirical models of surface duct propagation are useful in providing simple, realistic, quantitative estimates of the mean acoustic field in the duct and changes in the mean field due to changes in environmental conditions. As an example, the effect on the transmission loss due to duct leakage from an increase in sea-state by one value (a change from sea-state 2 to sea-state 3 etc) is equivalent to a nearly 50% increase in source/receiver range. However, changes in duct thickness have a negligible impact (as long as the sound frequency is significantly above the duct cut-off frequency), due to its competing effects on geometrical spreading and duct leakage. Numerical calculations of sound exposure using a semi-empirical surface duct model and simple models of the source and receiver motion indicate the importance of relative source/receiver speed and minimum source/receiver range to the total exposure.

In conclusion, the underwater sound fields created by human activities simultaneously and in the same region as the mass strandings of beaked whales examined in this paper appear to have several features in common. The actual relationship of these features with the strandings is unknown. A critical piece of information, the locations of the animals as a function of time, is missing for these events.

## ACKNOWLEDGEMENTS

We would like to acknowledge all the contributors to the D'Amico (1998) and the Fromm and McEachern (2000) reports for their efforts in understanding the acoustic propagation conditions during the 1996 Greek and Bahamas 2000 mass stranding events. The other members of the external review committee for the acoustic modelling effort in the Bahamas 2000 stranding event, Bill Kuperman, Jim Miller, Henrik Schmidt and Mike Collins deserve special thanks. Work on this project by Angela D'Amico and David Fromm was supported by the Office of Naval Research.

## REFERENCES

American National Standards Institute (ANSI). 1994. *Acoustical terminology: ANSI/ASA S1.1 – 1994 R1999*. American National Standards of the Acoustical Society of America. 52pp.

Anon. 2001. Joint interim report on the Bahamas marine mammal stranding event of 15-16 March 2000 (December 2001). *NOAA Tech. Mem.* :59pp. [Available at *http://www.nmfs.noaa.gov/prot_res/PR2/Health_and_Stranding_Response_Program/Interim_Bahamas_Report.pdf]*.

Baker, W.F. 1975. New formula for calculating acoustic propagation loss in a surface duct in the sea. *J. Acoust. Soc. Am.* 57(5):1198-200.

Brekhovskikh, L.M. and Lysanov, Y. 1991. *Fundamentals of Ocean Acoustics*. 2nd Edn. Springer-Verlag, New York. 270pp.

Collins, M.D. 1995. *User's Guide for RAM versions 1.0 and 1.0p*. Naval Research Laboratory, Washington, DC.

Cox, T.M., Ragen, T.J., Read, A.J., Vos, E., Baird, R.W., Balcomb, K., Barlow, J., Caldwell, J., Cranford, T., Crum, L., D'Amico, A., D'Spain, G., Fernández, A., Finneran, J., Gentry, R., Gerth, W., Gulland, F., Hilderbrand, J., Houser, D., Hullar, T., Jepson, P.D., Ketten, D., MacLeod, C.D., Miller, P., Moore, S., Mountain, D., Palka, D., Ponganis, P., Rommel, S., Rowles, T., Taylor, B., Tyack, P., Wartzok, D., Gisiner, R., Mead, J. and Benner, L. 2006. Understanding the impacts of anthropogenic sound on beaked whales. *J. Cetacean Res. Manage.* 7(3):In press.

D'Amico, A. and Verboom, W. 1998. Summary record and report of the SACLANTCEN Bioacoustics, Marine Mammal Policy, and Mitigation Procedures Panels, 15-19 June 1998. SACLANTCEN Marine Mammal Environmental Policy and SACLANTCEN Marine Mammal and Human Divers: Risk Mitigation Rules. (SACLANTCEN M-133, SACLANCT Undersea Research Center, La Spezia, Italy; 128pp)

Department of the Environment, G.of the C.I. 2002. Whale Stranding Special. Web page with information and reports on the September

2002 Canary Island stranding. (*http://www.gobcan.es/medioambiente/eng/varamientos.index.html*.)
Diebold, J., Webb, S., Tolstoy, M., Rawson, M., Holmes, C., Bohnenstiehl, D. and Chapp, E. 2003. R/V Ewing seismic source array calibrations: 2003. *EOS Trans. Am. Geophys. Un.* 84(46 (Fall meeting, supplement)):Abs OS41A-03.
Fisher, F.H. and Simmons, V.P. 1977. Sound absorption in sea water. *J. Acoust. Soc. Am.* 62:558-64.
Fontana, P. 2002. Seismic surveys and marine mammal protection. Presentation at IEEE Oceans 2002, Biloxi, MS, 29 October 2002.
Fox, D.N. 1996. *MODAS (Modular Ocean Data Assimilation System) Version 1.0*. Naval Research Lab, Stennis Space Center. Available from *http://www7300.nrlssc.navy.mil/html/mstrns.html* and *http://www7300.nrlssc.navy.mil/html/dart-home.html.*
Frantzis, A. 1998. Does acoustic testing strand whales? *Nature* 392(6671):29.
Friedman, N. 1989. *The Naval Institute Guide to World Naval Weapons Systems*. Naval Institute Press, Annaopolis, MD. 640pp.
Fromm, D.M. and McEachern, J.F. 2000. *Acoustic Modelling of the New Providence Channel*. US Office of Naval Research, Washington, DC. 56pp.
Gentry, R. 2002. URL: *http://www.noaa.gov.protres/PR2/HealthandStrandingResponseProgram/MassGalapagosIslands.htm.*
Hall, M. 1980. Surface-duct propagation: an evaluation of models of the effects of surface roughness. *J. Acoust. Soc. Am.* 67(3):803-11.
Jensen, F.B., Kuperman, W.A., Porter, M.B. and Schmidt, H. 1994. *Computational Ocean Acoustics*. American Institute of Physics, New York, NY. 612pp.
Kinsler, L., Frey, A., Coppens, A. and Saunders, J. 1982. *Fundamentals of Acoustics*. 3rd Edn. J. Wiley and Sons, Hoboken, New Jersey. 560pp.
Medwin, H. and Clay, C.S. 1998. *Fundamentals of Acoustical Oceanography*. Academic Press, London and San Diego. 712pp.
National Research Council. 2003. *Ocean Noise and Marine Mammals*. National Academic Press, Washington, DC. 192pp.
Norton, G., Novarini, J. and Keiffer, R.S. 1998. Modelling the propagation from a horizontally directed high frequency source in shallow water in the presence of bubble clouds and sea surface roughness. *J. Acoust. Soc. Am.* 103:3256-66.
Phillips, O.M. 1977. *Dynamics of the Upper Ocean*. 2nd Edn. Cambridge University Press, London. 344pp.
Pierson, W.J. and Moskowitz, L. 1964. A proposed spectral form for fully developed wind seas based on the similarity theory of S. Kitaigorodski. *J. Geophys. Res.* 69:5181-90.
Richardson, W.J., Greene Jr, C.R., Malme, C.I. and Thomson, D.H. 1995. *Marine Mammals and Noise*. Academic Press, San Diego. 576pp.
Sandwell, D., Smith, T., Smith, W.H.F. and Small, C. 1998. Measured and estimated seafloor topography. (Website: *http://topex.ucsd.edu/marine_topo/mar_topo.html*.)
Saunders, S. 2004. Table IX, Operational surface ship sonar equipments. *In:* S. Saunders (ed.) *Jane's Underwater Warfare Systems*. Jane's Information Group, *http://juws.janes.com*.
Schulkin, M. 1968. Surface-based losses in surface sound channels. *J. Acoust. Soc. Am.* 44(4):1152-4.
Socolovsky, J. 2002. NATO Exercise Neo Tapon 2002 causes mass whale beachings and deaths. AP story, 10 October 2002, located at *http://www.mindfully.org/Water/Neo-Tapon-Whale-Beaching10oct02.htm*.
Tolstoy, I. and Clay, C.S. 1987. *Ocean Acoustics: Theory and Experiment in Underwater Sound*. 2nd Edn. American Institute of Physics, New York.
Urick, R.J. 1979. *Sound Propagation in the Sea*. Defence Advanced Research Projects Agency, Washington, DC.
Urick, R.J. 1983. *Principles of Underwater Sound*. 3rd Edn. McGraw Hill, Baskerville, New York. xiv+423pp.
Weinberg, H. and Keenan, R.E. 1996. Gaussian ray bundles for modeling high-frequency propagation loss under shallow-water conditions. *J. Acoust. Soc. Am.* 100:1421-31.
Wenz, G.M. 1962. Acoustic ambient noise in the ocean: spectra and sources. *J. Acoust. Soc. Am.* 34(6):1936-56.

Date received: August 2004
Date accepted: August 2005